Physicochemical Characterization of Iron Oxide Nanoparticle Coated with Chitosan for Biomedical Application

**Tarfi Aziz[1*], Shah Md. Masum[1], Md. Rakibul Qadir[2], Abdul Gafur[2]
and Dilruba Huq[1]**

[1]*Department of Applied Chemistry and Chemical Engineering, Faculty of Engineering and
Technology, University of Dhaka, Bangladesh.*
[2]*Pilot Plant and Process Development Center, Bangladesh Council of Scientific and Industrial
Research, Dhaka, Bangladesh.*

Authors' contributions

This work was carried out in collaboration between all authors. Author TA performed the analysis,
wrote the protocol and the first draft of the manuscript. Authors SMM, AG and DH supervised the
research, helped with literature searches and provided the instrumental facilities. Author MRQ helped
to perform the XRD analysis. All authors read and approved the final manuscript.

Original Research Article

ABSTRACT

Aims: Synthesize and characterize a bio-polymer coated iron oxide nanoparticle, which has the
potency to be used as an appropriate biomaterial for biomedical purpose. Magnetic iron oxide
nanoparticles (MNPs) with biological coating exhibits many properties that can be exploited in a
variety of biomedical applications.
Place and Duration of Study: The study was performed at Bangladesh Council of Scientific and
Industrial Research (BCSIR), Dhaka, Bangladesh from August 2013 to August 2014.
Methodology: This research work describes the in-situ synthesis of chitosan-coated magnetic
nanoparticles (CS MNPs) by co precipitation method where trisodium phosphate is added as ionic

___

Corresponding author: E-mail: tarfi_aziz@yahoo.com ;

cross-linker. Analytical characterization of synthesized nanoparticles was performed using X-Ray Diffraction (XRD), Fourier Transform Infrared Spectroscopy (FTIR), Thermal gravimetric analysis (TGA) and Scanning Electron Microscope (SEM).

Results: The XRD analysis proved that the synthesized iron oxide was magnetite (Fe_3O_4). The layer of chitosan on the magnetite surface was confirmed by FTIR. SEM image demonstrated a comparable morphology. The average diameter of synthesized nanoparticle was found to be 13.4 nm from XRD crystallite size analysis. TGA result indicated that the chitosan content of CS MNP were 29% by weight.

Conclusion: The synthesized MNPs have many potential applications in biomedicine including targeted drug delivery, magnetic resonance imaging (MRI), and magnetic hyperthermia.

1. INTRODUCTION

Magnetic particles with dimensions ranging from the nanometer to the micrometer scales are being used in an increasing number of medical applications. The most important properties of magnetic particles for clinical diagnostics and medical therapies are nontoxicity, biocompatibility, injectability, and high-level accumulation in the target tissue or specific organ [1]. Magnetic iron oxide nanoparticles are the primary choice. The unique feature of MNPs to be guided by an external magnetic field has been used in magnetic resonance imaging (MRI), tissue repair, hyperthermia, drug delivery, and in cell separation [2,3,4,5]. Two other advantages of iron oxide nanoparticles are their low toxicity on cells and superparamagnetic properties. Superparamagnetic nanoparticles exhibit outstanding magnetic properties because they show no magnetization in the absence of a magnetic field but become strongly magnetized in the presence of magnetic field [6]. With the ability to utilize magnetic attraction and or specific targeting of disease biomarkers, MNPs offer an attractive means of remotely directing therapeutic agents specifically to a disease site while simultaneously reducing dosage and the deleterious side effects associated with non-specific uptake of cytotoxic drugs by healthy tissue [7]. For biomedical applications, iron oxide MNP must be precoated with substances that assure their stability, biodegradability, and non-toxicity in the physiological medium in order to achieve combined properties of high magnetic saturation, biocompatibility, and interactive functions on the surface [8]. Size and surface properties of iron oxide nanoparticles are the two important factors which could dramatically affect the nanoparticle efficiency as well as their stability. MNPs are preferred to be super-paramagnetic and have high magnetization

property so that their movement in the blood can be controlled with external magnetic field and be immobilized close to the targeted tissue [4]. Surfactants are used to coat magnetic nanoparticles which acts as a steric barrier to prevent aggregation caused by magnetic dipole–dipole attractions between particles and avoid opsonization [9]. In addition, polymeric coatings provide a means to tailor the surface properties of MNPs such as surface charge and chemical functionality [10]. The iron oxide core can be coated with polymers during the synthesis process and it must be a long chain. Among the coating materials studied to date, chitosan has drawn considerable attention. Chitosan, prevents the particles reacting with blood proteins and receptors [11].

In this study magnetic iron oxide nanoparticles were synthesized by the co-precipitation method because of its potential for large-scale manufacturing, cost-effectiveness, ease of production, and hydrophilicity of nanocrystals [12]. Hydrophilicity of nanoparticles is a key requirement for biomedical applications [13].

Chitosan, made from naturally occurring chitin, is a biodegradable, biocompatible, linear polysaccharide [14] and has many reactive functional groups that can serve as an anchor for conjugation of therapeutics, targeting ligands, and imaging agents [15]. In comparison with many other polymers, the chitosan backbone contains number of free amine groups, which allow binding of many agents. The chitosan coated IONPs have a remarkable heating effect which has great potential in hyperthermia therapy [16].

For biomedical applications, chitosan-coated magnetic nanoparticles (CS MNPs) are generally synthesized by in situ coating method which is

alkaline coprecipitation of Fe (II) and Fe (III) precursors in aqueous solutions of hydrophilic chitosan polymers. These polymers serve to limit the core growth of iron oxide during the preparation, and to stabilize via steric repulsions when the nanoparticles disperse in aqueous media [17]. The co-precipitation method involves the precipitation of iron salts in the presence of chitosan and trisodium phosphate, which acts as a cross linker. Trisodium phosphate cross links the adsorbed chitosan molecules to each other through the ionic interaction.

This work aims to evaluate the magnetic chitosan coated iron oxide nanoparticle for biomedical application. The prepared biocomposite was characterized by several analysis for comparative study.

2. MATERIALS AND METHODS

Iron (II) chloride tetrahydrate ($FeCl_2 \cdot 4H_2O$), iron (III) chloride hexahydrate ($FeCl_3 \cdot 6H_2O$), acetic acid (CH_3COOH), and ammonium hydroxide (NH_4OH) were obtained from Merck, Germany; chitosan (LMW, 84.57% deacetylated) and tri sodium phosphate were purchased from Sigma-Aldrich Chemie GmbH, Germany.

2.1 Synthesis of Iron Oxide Nanoparticle

Magnetic iron oxide nanoparticles (MNPs) were prepared by alkaline co-precipitation of ferrous chloride tetrahydrate, $FeCl_2 \cdot 4H_2O$ (1.34 g) and ferric chloride hexahydrate $FeCl_3 \cdot 6H_2O$ (3.40 g) at 1:2 ratio. The salts were dissolved in 150 mL deionized water within a three necked glass balloon. The glass balloon was placed in a heating mantle and stirred with a magnetic stirrer. It was vigorously stirred at 90ºC in the presence of N_2 gas. Ammonium hydroxide (NH_4OH) was added to the system drop wise. The process was ended by washing with deionized water until the solution pH was 9.0. The solution was then centrifuged at 5000 rpm for 30 minutes. The precipitates were collected and dried in the incubator at 55ºC. The black precipitates were then turned into brown.

2.2 Synthesis of Chitosan-coated Magnetic Iron Oxide Nanoparticles

Chitosan-coated magnetic iron oxide nanoparticles (CS MNP) were in situ synthesized by the co-precipitation of Fe (II) and Fe (III) salts in the presence of chitosan and trisodium phosphate molecules. Chitosan was previously prepared with degree of deacetylation 75% by titrimetric method [18,19]. Trisodium phosphate was used for the crosslinking of low molecular weight chitosan polymers. Chitosan (0.15 g) was dissolved in 30 ml of 1% acetic acid and the pH was adjusted to 4.8 by 10M NaOH. Iron salts (1.34 g $FeCl_2 \cdot 4H_2O$ and 3.40 g $FeCl_3 \cdot 6H_2O$) were dissolved in 30 ml of 0.5% chitosan solution. The solution was then vigorously stirred at 2000 rpm. 10 ml of 22.5% trisodium phosphate and different amounts of 32% NH_4OH (18, 20, 22, 25 mL) were added to the solution to obtain the final NH_4OH concentration of 31%, at room temperature. The ammonia solution was added very slowly to produce smaller sized nanoparticles. The resulting solution was stirred for an additional 1 hour. The colloidal chitosan coated magnetic Fe_3O_4 nanoparticles were extensively washed (3 times) with deionized water and separated by centrifugation and drying.

2.3 Analytical Characterization

Characterization of MNPs, chitosan biopolymers and CSMNPs were carried out by X-ray diffraction (XRD), Fourier Transformed Infrared Spectroscopy (FTIR) and Laser Diffraction Particle Size Analyzer.

2.3.1 X-ray diffraction (XRD)

X-ray diffractometer (XRD) (D8 ADVANC, BRUKERE AXS GmbH, Germany) was used to investigate the mineral phase of obtained materials. XRD measurements were performed with Cu Kα radiation ($λ$ = 1.54178 Å), with the operation voltage and current at 40 kV and 40 mA, respectively. The 2θ range was from 5°-90° in steps of 0.02°.

2.3.2 Fourier transformed infrared spectroscopy (FTIR)

The FTIR spectroscopy of the sample was taken in the region between 500-4000 cm^{-1} (with Perkin Elmer 1650, USA) on a Thermo-Nicolet Avatar 370 model FTIR in order to understand the chemical and structural nature of the Chitosan coated iron oxide nanoparticle.

2.3.3 Laser diffraction particle size analyzer

Particle size of bare MNP and CSMNP were determined by using Laser Diffraction particle Size Analyzer (Microtrac Model S3500, USA).

2.3.4 Thermo-gravimetric analysis /differential thermal analysis/derivative thermo-gravimetric analysis (TG/DTA/DTG)

TGA shows the change in mass with the increase of temperature. This studies were carried out by TG/DTA 6300, SII Nano Technology, Japan by heating the sample at 20ºC /min in the temperature range 100ºC - 1000ºC in nitrogen atmosphere.

2.3.5 Morphological analysis of the CSMNP

The size of the prepared sample (CSMNP) was related to properties such as bioavailability and surface modification for in vivo application. The particles were inspected with Scanning Electron Microscopy (SEM, model: JEOL JSM-6490LA) to identify average diameter, interconnectivity, and any agglomeration.

3. RESULTS AND DISCUSSION

In the synthesis of bare MNPs (Fig. 1b), pure Fe_3O_4 (Fig. 1a) were formed at the temperature of 90ºC. The characteristic properties of synthesized bare and CSMNPs (Fig. 1c) have been analyzed by various analytical methods.

Crystal structures of synthesized MNPs were analyzed by XRD. The chemical groups and chemical interactions involved in synthesized MNPs were identified using the FTIR methods. The sizes of magnetic core and morphological properties were observed through SEM images. The qualitative and quantitative information about the volatile compounds of CSMNP were performed using TGDTA.

3.1 XRD

Fig. 2a shows the XRD pattern of synthesized crystalline iron oxide (Fe_3O_4) nanoparticle. Fe_3O_4 exhibits a strong and sharp peak in the diffarctogram. The diffraction peaks are obtained at (220), (311), (400), (422), (511), and (440), which are the characteristic peaks of magnetite (Fe_3O_4). The peaks in the XRD patterns of iron

oxide are compared with the standards, (JCPDS card file no 77-1545), appeared in both bare and chitosan coated iron oxide nanoparticle. The diffractogram of chitosan are showed in Fig. 2a&c, which revealed the characteristic peak between 9º-20º with comparable degree of crystallinity (Fig. 2a) [20,21]. The XRD spectrum of chitosan is reported in various literature which shows peaks with low intensity values around $2\theta=10º$ and a broad peak at around $2\theta=15º-35º$. XRD result exposed a broader peak in chitosan coated iron oxide nanoparticle (CSMNP), which indicates the smaller crystallite size of the produced CSMNP than that of the starting iron oxide nanoparticles and this may be devoted to the method of preparation of composite which causes the coating of chitosan on iron oxide nanoparticle.

The crystallite size of both iron oxide and produced composite (CSMNP) were calculated from peaks at $2\theta = 35.55º$ corresponding to iron oxide phase using Scherrer Equation [22].

$$D_p = \frac{0.94\lambda}{\beta_{1/2}\cos\theta}$$

In the equation, β is the FWHM of diffraction peak, λ is the wave length of X-ray (0.154 nm), L is the crystallite size, and θ is the Bragg peak position. The crystallite size was found to be 13.4 nm and 11.6 nm for both MNP and CSMNP respectively.

3.2 FTIR

The chemical composition of synthesized nanoparticles was confirmed by the FTIR. The FTIR results were given with their auto baseline corrections. The presence of Fe_3O_4 core could be identified by the strong stretching absorption band at 581.55 cm^{-1}, which corresponded to the Fe-O. The peak located in the 570 cm^{-1} region was found in bare and chitosan coated nanoparticle spectra (Fig. 3), which confirmed that the product contained magnetite.
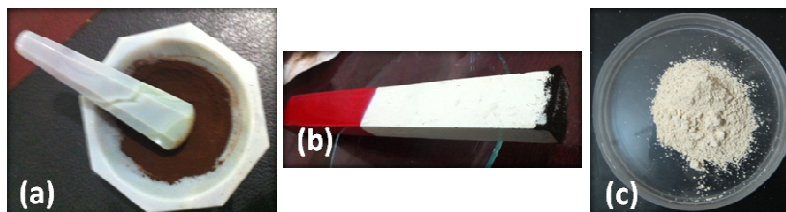

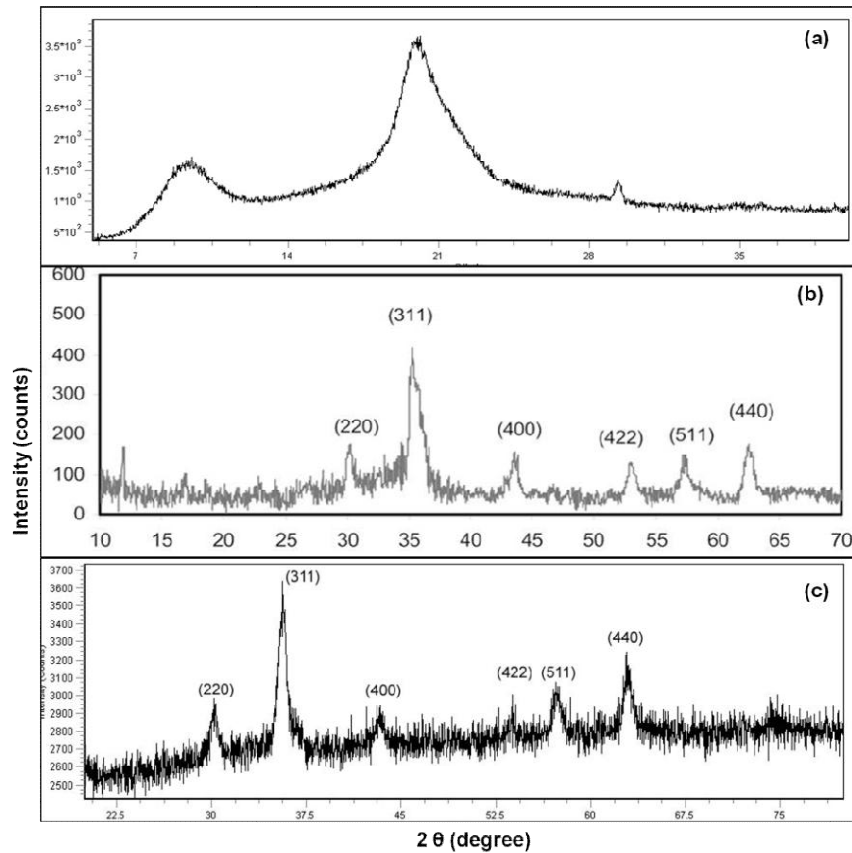**Fig. 1. Pure iron oxide (a) bare magnetic nanoparticle (b) and CSMNP (c)**

Fig. 2. XRD pattern of synthesized crystalline iron oxide (Fe$_3$O$_4$) nanoparticle (a) chitosan (b) and CSMNP (c)
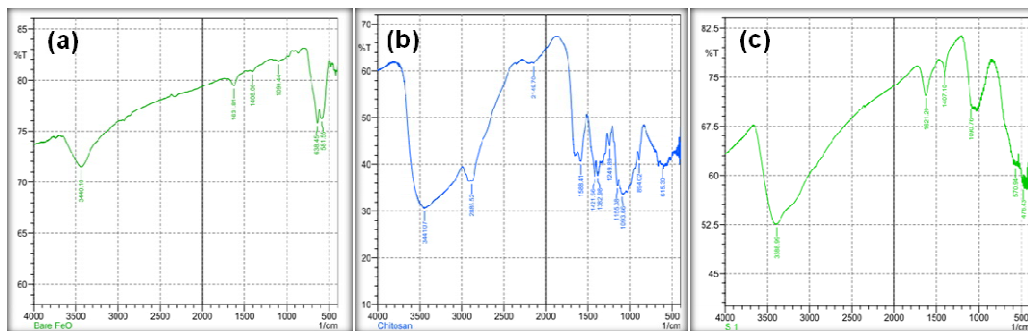

Fig. 3. FTIR spectra of bare MNP (a), chitosan (b) and CSMNP (c)

The peaks around 1621.20 cm^{-1}, assigned to the -NH2 group bend scissoring, are present in both chitosan and chitosan coated nanoparticle spectra, which proved that the magnetite nanoparticles were successfully coated by chitosan polymer [23]. In the IR spectrum of chitosan (Fig. 3b), the band at 1588.41 cm^{-1} was assigned to –NH2 group bend scissoring, the peak at 1421 cm^{-1} to OH bending of primary alcoholic group, and 1155.38 cm^{-1} to C-N stretch in chitosan. In the spectrum of CS MNP S1 (Fig. 3c), the 1588.41cm^{-1} peak of –NH2 bend scissoring in chitosan, shifted to 1621.20 cm^{-1} and a new peak at 570.94 cm^{-1} was appeared. All characteristic peaks of chitosan and iron oxide were present in the spectrum of CSMNPs. Similar results were also observed in [24,25].

3.3 Particle Size Analysis

The particle size analysis curve (Fig. 4) showed the particle sizes as a frequency distribution or histogram (% channel) and a cumulative distribution (% passing). The X axis label represents the particle diameter in nanometer (nm). More than 75% of the particles obtained a size of 240 nm for both bare magnetic nanoparticle (Fig. 4a) and CSMNP (Fig. 4b). The particle size and shape obtained varied due to the presence of agglomeration which was also observed by other researchers [26,27,28].

3.4 Thermal Gravimetric Analysis

The TGA–FTIR analysis of bare and chitosan-coated Fe_3O_4 nanoparticles provides qualitative and quantitative information about the volatile components of the nanoparticles. The TGA curve shows that the weight loss of bare MNPs over the temperature range from 50ºC to 950ºC is about 7%. This might be because of the loss of residual water in the sample. The CSMNPs gave

their distinctive TGA curves, which can provide indications of the content of chitosan polymers [29]. The principle chains of chitosan began to degrade at about 210ºC and the final temperature of decomposition was around 600ºC (Fig. 5).

The results of TGA-DTGA demonstrated that most of the organic layer, chitosan, was removed as CO_2 at high temperatures. TGA result indicated that the chitosan content increased at higher temperature and maximum amount is found about 29% by weight.

3.5 Scanning Electron Microscopy (SEM)

Fig. 6 represents the SEM image of Chitosan coated iron oxide nanoparticle obtained by coprecipitation method. The SEM image at 100,000X magnifications was collected. From the SEM image of CSMNP, it was observed that the particles are well-dispersed spherical, accompanying almost well-defined and uniform crystalline structure (Fig. 6).
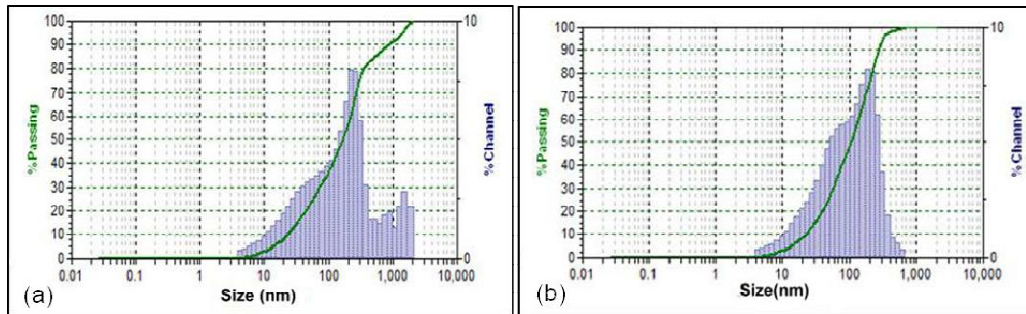

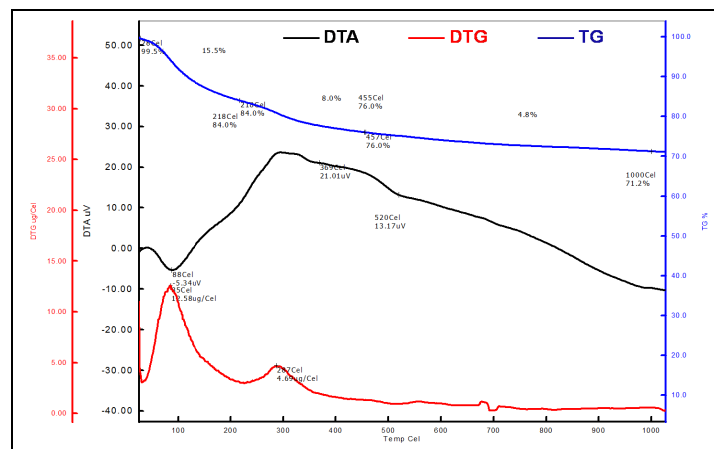**Fig. 4. Particle size distribution for bare MNP (a) and CSMNP (b)**

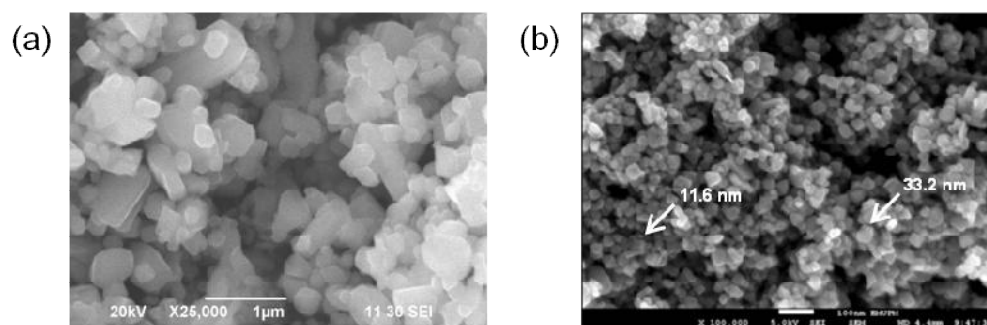**Fig. 5. TG, DTG, and DTA curve of bare iron oxide nanoparticle**

Fig. 6. The SEM image of bare MNP (a) and CS MNP (b)

There was also a higher tendency of agglomerations. The island growth of the tightly packed spherical arrangement was clearly observed. In some regions, the big nanoparticles were surrounded by smaller nanoparticles. The average diameter measured is about 22.4 nm which is nearly in agreement with the particle size obtained from XRD analysis. Similar result is also found from [30,31].

4. CONCLUSION

The synthesis of nanoparticles with small size and uniform size distribution is a subject of intensive research in recent years. In this study Chitosan polymer was coated on iron oxide core by ionic-cross linking of trisodium phosphate. Size-tunable synthesis of chitosan-coated magnetic nanoparticles by in situ coprecipitation method at this small size range is very recently been reported. This method is advantageous than the earlier published methods [32] because the process is simple and carried out under mild conditions without using hazardous organic solvents. The nanoparticles obtained by our method are expected to have better biocompatibility than covalently cross-linked chitosan [33,34] as the chitosan was cross-linked with ionic interactions.

The XRD pattern indicated crystalline structure of iron oxide nanoparticle and the coating with chitosan resulted a noisy amorphous peak because chitosan raw material is essentially non-crystalline [19]. The crystallite size obtained from X-Ray powder diffraction is about 13.4 nm which successfully conforms to the biological application. The SEM image of CSMNPs showed that the particles were spherical. The FTIR spectra confirmed the presence of metal-oxygen bond. Further studies will be done for antimicrobial analysis and cytotoxicity assay to check its bioavailability.

COMPETING INTERESTS

Authors have declared that no competing interests exist.

REFERENCES

1. Ito A, Shinkai M, Honda H, Kobayashi T. Medical application of functionalized magnetic nanoparticles. J Biosci Bioeng. 2005;100(1):1-11.

2. Mornet S, Vasseur S, Grasset F, Veverka P, Goglio G, Demourgues A, Portier J, Pollert E, Duguet E. Magnetic nanoparticle design for medical applications. Prog Solid State Chem. 2006;34:237-247.

3. Gupta AK, Gupta M. Synthesis and surface engineering of iron oxide nanoparticles for biomedical applications. Biomaterials. 2005;26:3995-4021.

4. Gupta AK, Wells S. Surface-modified superparamagnetic nanoparticles for drug delivery: Preparation, characterization, and cytotoxicity studies. NanoBioscience, IEEE Transactions on. 2004;3(1):6673.

5. McCarthy JR, Kelly KA, Sun EY, Weissleder R. Targeted delivery of multifunctional magnetic nanoparticles. Future Med; 2007.

6. Corrot C, Robert P, Idee JM, Port M. Recent advances in iron oxide nanocrystal

technology for medical imaging. Adv. Drug Deliver. Rev. 2006;58:1471-1504.

7. Alexiou C, Arnold W, Hulin P, Klein RJ, Renz H, Parak FG, Lübbe AS. Magnetic mitoxantrone nanoparticle detection by histology, X-ray and MRI after magnetic tumor targeting. J Magnetism and Magnetic Mat. 2001;225(1):187-193.

8. Tartaj P, del Puerto Morales M, Veintemillas-Verdaguer S, Gonzalez-Carreno T, Serna CJ. The preparation of magnetic nanoparticles for applications in biomedicine. J Physics D: App Physics. 2003;36(13):R182.

9. Denkbaş EB, Kiliçay E, Birlikseven C, Öztürk E. Magnetic chitosan microspheres: Preparation and characterization. Reactive and Functional Polymers. 2002;50(3):225-232.

10. Berry CC, Curtis ASG. Functionalisation of magnetic nanoparticles for applications in biomedicine. J Phy D: App Physics. 2003;36:R198-R206.

11. Weissleder R, Bogdanov A, Neuwelt EA, Papisov M. Long-circulating iron oxides for MR imaging. Adv Drug Delivery Rev. 1995;16:321-334.

12. Qu S, Yang H, Ren D, Kan S, Zou G, Li D, Li M. Magnetite nanoparticles prepared by precipitation from partially reduced ferric chloride aqueous solutions. J Colloid and Interface Sci. 1999;215:190-192.

13. Massart R, Cabuil V. Effect of some parameters on the formation of colloidal magnetite in alkaline-medium-yield and particle-size control. Journal de Chimie Physique et de Physico-Chimie Biologique. 1987;84(7-8):967-973.

14. Chung HJ, Go DH, Bae JW, Jung IK, Lee JW, Park KD. Synthesis and characterization of Pluronic® grafted chitosan copolymer as a novel injectable biomaterial. Current Applied Physics. 2005;5:485-488.

15. Kim DK, Zhang Y, Voit W, Rao KV, Muhammed M. Synthesis and characterization of surfactant-coated superparamagnetic monodispersed iron oxide nanoparticles. J Magnetism and Magnetic Mat. 2001;225:30-36.

16. Qu Y, Hua J, Tian H. Colorimetric and ratiometric red fluorescent chemosensor for fluoride ion based on diketopyrrolopyrrole. Organic letters. 2010;12(15):3320-3323.

17. Mornet S, Vasseur S, Grasset F, Duguet E. Magnetic nanoparticle design for medical diagnosis and therapy. J Mat Chem. 2004;14(14):2161-2175.

18. Nessa F, Masum SM, Asaduzzaman M, Roy SK, Hossain MM, Jahan MS. A process for the preparation of chitin and chitosan from prawn shell waste. Bangladesh J Scientific and Indust Res. 2010;45(4):323-330.

19. Kabiraj MK, Jahan IA, Masum SM, Islam MM, Hasan SMM, Saha B, Nur HP. Effective Removal of Chromium (VI) Ions from Tannery Effluent using Chitosan-Alumina Composite. Int Res J Pure Appl Chem. 2015;10(3):1-12.

20. Li MC, Liu C, Xin M, Zhao H, Wang M, Feng Z, Sun X. Preparation and characterization of acylated chitosan. Chem Res Chinese U. 2005;21(1):114-116.

21. Lu G, Kong L, Sheng B, Wang G, Gong Y, Zhang X. Degradation of covalently cross-linked carboxymethyl chitosan and its potential application for peripheral nerve regeneration. Eur Polym J. 2007;43:3807-3818.

22. Patterson AL. The Scherrer formula for X-ray particle size determination. Physical rev. 1939;56(10):978.

23. Coates J. Encyclopedia of analytical chemistry. In: Me-yers RA, (ed), Interpretation of infrared spectra, a practical approach. Wiley, Chichester. 2000;10815-10837.

24. Ma L, Gao C, Mao Z, Zhou J, Shen J, Hu X, Han C. Collagen/chitosan porous scaffolds with improved biostability for skin tissue engineering. Biomaterials. 2003; 24(26):4833-4841.

25. Zhang M, Smith A, Gorski W. Carbon nanotube-chitosan system for electrochemical sensing based on dehydrogenase enzymes. Analyt Chem. 2004;76(17):5045-5050.

26. Li G, Jiang Y, Huang K, Ding P, Chen J. Preparation andproperties of magnetic Fe_3O_4–chitosan nanoparticles. J Alloy Compd. 2008;66:451-456.

27. Dung DTK, Hai TH, Phuc LH, Long BD, Vinh LK, Truc PN. Preparation and characterization of magnetic nanoparticles with chitosan coating, APCTP–ASEAN Workshop on Advanced Materials Science and Nano-technology (AMSN08) IOP Publishing J of Physics, Conference Series. 2009;187:012036.

28. Zhang L, Zhu X, Sun H, Chi G, Xu J, Sun Y. Control synthesis of magnetic Fe3O4–

chitosan nanoparticles under UV irradiation in aqueous system. Curr Appl Phys. 2010;10:828-833.

29. Paama L, Pitkänen I, Halttunen H, Perämäki P. Infrared evolved gas analysis during thermal investigation of lanthanum, europium and samarium carbonates. Thermochimica Acta. 2003;403(2):197-206.

30. Shrifian EA, Salhi MT, Mojtaba NE, Ekramian E. Chitosan-modified superparamgnetic iron oxide nanoparticles: design, fabrication, characterization and antibacterial activity. CHEMIK. 2015;69(1):19-32.

31. Ali A, Muhammad MTM, Sijam K, Siddiqui Y. Effect of chitosan coatings on the physicochemical characteristics of Eksotika II papaya (*Carica papaya* L.) fruit during cold storage. Food Chemistry. 2011;124(2):620-626.

32. Tiaboonchai W, Limpeanchob N. Formulation and characterization of amphotericin B-chitosan-dextran sulfate nanoparticles. Int J Pharm. 2007;329:142-149.

33. Agnihotri SA, Mallikarjuna NN, Aminabhavi TM. Recent advances on chitosan-based micro and nanoparticles in drug delivery. J Cont Release. 2004;100(1):5-28.

34. Park JH, Saravanakumar G, Kim K, Kwon IC. Targeted delivery of low molecular drugs using chitosan and its derivatives. Adv Drug Deliv Rev. 2010;62:28-41.

Peer-review history:
The peer review history for this paper can be accessed here:
http://sciencedomain.org/review-history/12868